Computational modeling of combustion instabilities in lean premixed turbulent combustors

Bjørn Lilleberg, Ivar S. Ertesvåg* and Kjell Erik Rian

Department of Energy and Process Engineering
Norwegian University of Science and Technology
∗ e–mail: Ivar.S.Ertesvag@ntnu.no

Summary   In this work the reaction-rate response of different species to inlet flow variations have been studied using an unsteady perfectly stirred reactor model. Transient simulations of variations in mass flow rate, temperature and mixture equivalence ratio at the reactor inlet have been conducted. Combustion of methane and propane, with both global single-step and detailed chemical kinetic mechanisms, has been simulated. The detailed mechanisms predict similar general trends. The global and detailed mechanism for methane predict almost the same reaction rates, whereas the predicted reaction rates from the global and detailed mechanism for propane are very different at high equivalence ratios, near stoichiometry. The reaction-rate oscillations were not very sensitive to imposed small oscillations on the inlet temperature. An imposed small oscillation on the inlet mass flow rate gave reaction-rate oscillations that were almost constant at both rich and lean mixtures. The largest variations in reaction rate oscillations between rich and lean mixtures were found when imposing a small oscillation on the equivalence ratio of the mixture at the inlet. The present study indicates that variations in the inlet mixture equivalence ratio may lead to combustion instabilities in lean premixed combustion.

Keywords: combustion, instabilities, lean premixed, chemical kinetics, PSR, equivalence ratio

Introduction

More stringent emission regulations drive the new generation of gas turbines to leaner premixed operation in order to lower the combustion temperature and thereby the NO_x formation. The thermal NO_x mechanism is mainly a function of flame temperature and residence time. In contrast to non-premixed systems, lean premixed systems allow the majority of the fuel to be burned at lower temperatures, and hence, producing less NO_x. However, lean premixed combustors are susceptible to thermoacoustic oscillations and other instabilities. These combustion instabilities are characterized by oscillations of one or more natural acoustic modes of the combustor. The driving mechanism behind these instabilities in gas turbine combustors are generally caused by complex feedback-type interactions between a periodic flow field, chemical kinetics, heat release, acoustics and pressure fluctuations. However, the details of the mechanisms leading to amplification, self-sustenance and damping of the oscillations is not very well understood. These combustion instabilities are recognized by system vibrations, enhanced heat transfer and thermal stresses to the combustors walls and flame blowoff or flashback [1].

In the present study an in-house code using an unsteady perfectly stirred reactor (PSR) model has been developed to investigate the role of unmixedness and chemical kinetics in driving combustion instabilities of lean premixed combustion. This work is a continuance of the work reported by Lieuwen et al. [2] who studied the transient development of reaction-rate oscillations produced by periodic flow rate, temperature and equivalence ratio variations in the combustor inlet flow at different mean equivalence ratios. They used an unsteady well stirred reactor (WSR) model which is exactly the same as an PSR. Their study was partly motivated by the work of Shih et al. [3] and Cohen and Anderson [4]. Shih et al. [3] studied the influence of reactant unmixedness on combustion stability. They found that instabilities occured near

stoichiometric conditions, whereas for lean mixtures the combustor was stable. On the other hand, Cohen and Anderson [4] found that the amplitude of the pressure oscillations increased as the combustor was operated at leaner mixtures. Using a global single-step kinetic mechanism for propane, Lieuwen et al. [2] concluded that periodic variations in equivalence ratio play a key role in driving combustion instabilities for lean premixed conditions. Prior to the present study, some preliminary investigations on combustion instabilities have also been performed by Myhrvold and Gruber [5].

In the present work the response of the model to variations in flow rate, temperature and equivalence ratio have been tested. Moreover, the global chemical kinetic mechanism used by Lieuwen et al. [2] for propane and a detailed kinetic mechanism for propane are compared, and the same is done for methane.

Reactor modeling

From a combustion regime diagram for turbulent premixed combustion, see e.g. [6, 7], it is observed that the well/perfectly stirred reactor regime represents fast turbulent mixing where the characteristic times of the turbulent motions are shorter than the chemical reaction time. In an unsteady perfectly stirred reactor (PSR) model, which is an ideal reactor model, perfect mixing is achieved instantaneously inside the combustor, and the properties inside the combustor are uniform, i.e. no spatial gradients [8]. Typically, modeling premixed combustion as a PSR makes it possible to isolate the effects of the chemical kinetics. Furthermore, the details of the convection and mixing processes are neglected. The governing equations for the PSR model can be stated as follows

$$\frac{dY_i}{dt} = \frac{1}{\tau}(Y_{i,\text{in}} - Y_i) + \frac{R_i}{\rho} \qquad i = 1, \ldots, N_\text{S} \tag{1}$$

$$\frac{dh}{dt} = \frac{1}{\tau}(h_{in} - h) + Q \tag{2}$$

$$\frac{dp}{dt} = 0 \tag{3}$$

and $1/\tau$ is defined as

$$\frac{1}{\tau} = \frac{\dot{m}_\text{in}}{m_\text{R}} = \frac{\dot{m}_\text{in}}{(\rho \cdot V_\text{R})} \tag{4}$$

where $\rho = \rho(T, Y_i, p)$ and $R_i = R_i(T, Y_i, p)$. Here, t, Y_i, h, p, ρ, T, R_i and Q refer to time, species mass fraction, specific enthalpy, pressure, mass density, temperature, species volumetric reaction rate and heat transfer, respectively. Index i refers to chemical species, N_S is the number of species and subscript "in" refer to conditions at the reactor inlet. τ is the reactor residence time and $\dot{m}_\text{in}$, m_R and V_R are the mass flow rate into the reactor, the mass inside the reactor and the reactor volume, respectively. The perfectly stirred reactor is shown in Fig. 1. Equations (1)-(3) of the PSR model are the same as those used in the Eddy Dissipation Concept for turbulent combustion [7] for detailed chemistry calculations. Lieuwen et al. [2] also used an unsteady PSR model similar to Eqs. (1)-(3), but they expressed the energy balance, Eq. (2), in terms of the mixture temperature, T. In this work, an equation for the mixture enthalpy is used, and the mixture temperature is found from the mixture enthalpy and composition by Newton iteration. In order to obtain results that are independent of geometry-specific system dynamics, no feedback was included in the PSR model. This open-loop response of the combustor to inlet flow variations makes the results more general.
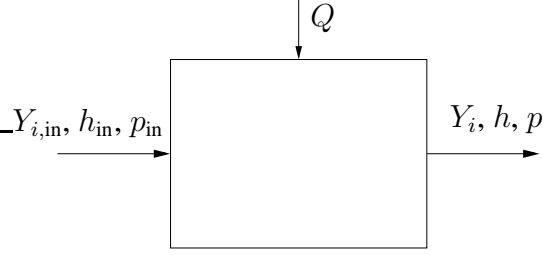
Figure 1: Perfectly stirred reactor

Regarding the reactor residence time, τ, there are different combinations of what could be held constant, see Table 1. In this study we have chosen to restrict the investigation to Mode I, as in the work of Lieuwen et al. [2].

Table 1: Various combinations of constants and variables in the τ-expression (see Eq. (4))

Mode	Constants	Variables	Extra information needed
I	$V_R, \dot{m}_{in}$	$m_R = \rho V_R \sim \rho, \tau \sim m_R \sim \rho$	No
II	V_R, τ	$m_R = \rho V_R \sim \rho, \dot{m}_{in} = m_R/\tau \sim \rho$	No
III	$\tau, \dot{m}_{in}, m_R = \tau \dot{m}_{in}$	$V_R = m_R/\rho \sim 1/\rho$	No
IV	$\dot{m}_{in}$	V_R, m_R, τ	dV_R/dt
V	τ	$V_R, m_R, \dot{m}_{in}$	dV_R/dt
VI	m_R	$V_R, \tau, \dot{m}_{in}$	dV_R/dt
VII	V_R	$m_R, \tau, \dot{m}_{in}$	dV_R/dt

Present predictions

General assumptions

The integration of Eqs. (1)-(3) is done with the implicit Runge Kutta code RADAU5, which is L-stable and of fifth order [9, 10]. The pressure in the PSR was set to be constant, $p = p_{in} = 1.0$ atm. The reactor was regarded as adiabatic ($Q = 0$).

Chemical mechanisms

In the present work, unsteady PSR simulations of methane-air and propane-air combustion have been studied using both global single-step and detailed finite-rate chemical mechanisms. For the single-step methane (CH_4) and single-step propane (C_3H_8) chemistry the chemical reaction rates can be written respectively as [2, 8, 11, 12, 13]

$$R_{CH_4} = 1.4704 \cdot 10^{12} \cdot \rho^2 \cdot Y_{CH_4} \cdot Y_{O_2} \cdot \exp(-17404.0/T) \tag{5}$$

$$R_{C_3H_8} = 4.773 \cdot 10^8 \cdot \rho^{1.75} \cdot Y_{C_3H_8}^{0.1} \cdot Y_{O_2}^{1.65} \cdot \exp(-15098.0/T) \tag{6}$$

According to [11] the computed flammability limits for the global single-step propane mechanism are $\phi_{lean} = 0.5$ and $\phi_{rich} = 3.2$. For the detailed chemistry calculations, GRI-Mech 3.0 [14] was used for the methane-air combustion and the San-Diego mechanism [15] was used for the propane-air combustion. CHEMKIN subroutines [16] were applied for the calculation of the chemical reaction rates from the detailed mechanisms. For all cases thermochemical data were

evaluated using CHEMKIN subroutines [16] and thermochemical data distributed with GRI-Mech 3.0 [14] and the San-Diego mechanism [15].

Validation of the reactor model

Initial tests of the numerical code developed for doing simulations with the unsteady PSR model have been done. These tests were performed by specifying the inlet flow properties, temporarily increasing the inlet flow temperature until ignition of the mixture, letting the inlet flow temperature drop back to 300 K, and then integrating in time until a steady-state solution were reached. Details of the ignition procedure are explained in the next section. The equivalence ratio of the mixture was varied between 1.0 and 0.7. All the chemical kinetic mechanisms were tested. The steady-state reactor temperature, T, and mixture composition, Y_i, were compared to results from a STANJAN [17] equilibrium calculator. The STANJAN equilibrium calculator performs calculations on a closed PSR (i.e. infinite residence time). The equilibrium calculations of the different fuel-air (21% O_2 and 79% N_2) mixtures were done with constant enthalpy and pressure (1 atm), which is the same as in the PSR numerical code. The additional species in the STANJAN calculations were CO_2 and H_2O for the global single-step mechanisms. For the detailed mechanisms the species from the PSR calculations were sorted from largest to smallest mole fraction and included in the STANJAN calculations until all fields were filled up. In the STANJAN calculator used in this work, 30 additional species could be added.

Ignition and extinction

The transient performance of the numerical code was tested by simulating ignition and extinction of the reactor. In these simulations the inlet flow temperature was a function of time [2]

$$T_{\text{in}} = \begin{cases} 300 + a \cdot t \cdot (0.025t - t^2) \text{ K} & \text{for} \quad 0 < \ t < 0.011 \text{ s} \\ 300 \text{ K} & \text{for} \qquad t \geq 0.011 \text{ s} \end{cases} \qquad (7)$$

Table 2 gives the different values of the constants a in Eq. (7) according to the respective fuel and mechanism used. The inlet equivalence ratio was also a function of time [2]

$$\phi_{\text{in}} = \begin{cases} 1.0 & \text{for} \quad 0 < \ t < 0.025 \text{ s} \\ 1.4 - 16 \cdot t & \text{for} \qquad t \geq 0.025 \text{ s} \end{cases} \qquad (8)$$

Table 2: Values of a in Eq. (7)

Mixture	Mechanism	Constant a
Propane-air	Single-step	$4.5 \cdot 10^6$
Propane-air	San-Diego	$6.8 \cdot 10^6$
Methane-air	Single-step	$3.2 \cdot 10^6$
Methane-air	GRI-Mech 3.0	$8.2 \cdot 10^6$

For these simulations the reactor pressure, p, and the ratio $\dot{m}_{\text{in}}/V_{\text{R}}$ were kept constant at 1 atm and 500 kg/(m³s), respectively (cf. Eq. (4)).

Periodic variations of the PSR inlet

Following the investigations made in [2], simulations of periodic variations of the PSR inlet were performed by varying the inflowing equivalence ratio, temperature and mass flow rate.

In four different cases the equivalence ratio, temperature and mass flow rate was periodically varied, respectively, as

$$\phi_{in} = \bar{\phi}_{in} \cdot (1.0 + 0.025 \cos(200 \cdot \pi \cdot t)) \tag{9}$$

$$\phi_{in} = \bar{\phi}_{in} \cdot (1.0 + 0.05 \cos(200 \cdot \pi \cdot t)) \tag{10}$$

$$T_{in} = 300.0 \cdot (1.0 + 0.05 \cos(200 \cdot \pi \cdot t)) \text{ K} \tag{11}$$

$$\dot{m}_{in}/V_R = 500.0 \cdot (1.0 + 0.05 \cos(200 \cdot \pi \cdot t)) \text{ kg/(m}^3\text{s)} \tag{12}$$

For all these simulations, first the stoichiometric mixture was ignited and then the mean equivalence ratio of the inlet flow, $\bar{\phi}_{in}$, was linearly reduced from $\bar{\phi}_{in} = 1.0$ (at $t = 0.05$ s) to $\bar{\phi}_{in} = 0.73$ (at $t = 0.4$ s) to allow the PSR to respond in a quasi-steady manner [2]. Table 3 shows how the PSR was operated during the four cases.

Table 3: operation of the the PSR during variation simulations, see Eqs. (9)-(12)

Case	Constant			Variation	
1	$P = 1$ atm,	$T_{in} = 300$ K,	$\dot{m}_{in}/V_R = 500$ kg/(m^{3}s)	ϕ_{in}	Eq. (9)
2	$P = 1$ atm,	$T_{in} = 300$ K,	$\dot{m}_{in}/V_R = 500$ kg/(m^{3}s)	ϕ_{in}	Eq. (10)
3	$P = 1$ atm,		$\dot{m}_{in}/V_R = 500$ kg/(m^{3}s)	T_{in}	Eq. (11)
4	$P = 1$ atm,	$T_{in} = 300$ K		$\dot{m}_{in}/V_R$	Eq. (12)

For propane the global mechanism Eq. (6) and the San-Diego mechanism [15] are compared, and for methane the global mechanism Eq. (5) and the GRI-Mech 3.0 [14] are compared. These comparisons are made for all of the four cases in Table 3.

Each of the variations shown in Table 3 and Eqs. (9)-(12) has an amplitude of 5 % about its mean value, except for Case 1 (ϕ_{in}, 2.5 % amplitude). Here, Case 1 corresponds to the results shown graphically in [2].

Results

Validation of the reactor model

In the initial reactor tests of the propane-air and methane-air mixtures with their respective mechanisms, the equilibrium solution obtained with the unsteady PSR numerical code (setting $\tau = 1.0$ s) showed very good agreement with the STANJAN equilibrium calculator (not presented here). The maximum temperature difference between the STANJAN calculations and the PSR calculations was 5.6 K. However, the global single-step propane mechanism failed to work for $\phi < 1.0$ with $\tau = 1.0$ s. For $\phi = 0.90$, the residence time τ had to be set to approximately $7 \cdot 10^{-4}$ s in order to avoid integrator failure.

Ignition and extinction

Figure 2 shows the results of the ignition and extinction simulations. It is observed that the PSR temperature, T, follows the inlet flow temperature until ignition, reaches a steady-state and then is reduced according to the subsequent reduction in the inlet equivalence ratio, ϕ_{in}. When the mixture reaches the lean limit, the reactor extinguishes and T drops towards T_{in}. Comparing the present results, using the global single-step propane mechanism, and the equivalent simulations by Lieuwen et al. [2] shows a qualitatively good accordance in general. There is, however, a difference in the predicted temperature and extinction time. The PSR temperature reported in [2]

is lower than that predicted in this work, and hence, the higher temperature delays the extinction. In [2] a steady-state temperature (for $\phi_{\text{in}} = 1.0$) of approximately 1950 K was predicted, whereas the corresponding temperature found here is approximately 2170 K. A possible reason for the lower temperature in [2] may be that their c_{p}-values were higher.

For $t > 0.025$ s, when making the inlet mixture to the reactor fuel-leaner (cf. Eq. (8)), we observe a small increase in T when using the single-step propane mechanism. This increase occurs because there is unburned propane in the reactor until ϕ_{in} is reduced to approximately 0.85 (at $t = 0.035$ s). After this, almost all the propane was consumed and the burned mixture is cooled by the excess air. The results of the San-Diego mechanism does not show this increase in temperature. Overall, as Fig. 2 a shows, the San-Diego mechanism predicts a lower temperature and extinction occurs earlier than for the single-step mechanism. By doing a STANJAN equilibrium calculation for propane, the maximum adiabatic flame temperature were found at $\phi = 1.05$ (rich mixture) [8]. Increasing ϕ_{in} from 1.0 to 1.1 (using $\tau = 1.0$ s) the San-Diego mechanism also showed a peak in temperature at $\phi_{\text{in}} = 1.05$, whereas the global single-step propane mechanism only showed a decrease in T for all these values of ϕ_{in}.

For the simulations of the methane-air mixtures we see the same qualitative behavior of the unsteady PSR model, see Fig. 2 b. Using the single-step kinetic mechanism for methane, there is no increase in T as the mixture is made leaner. Almost all the methane was consumed at the steady-state stage. Also for methane-air combustion, the temperature predicted with the single-step mechanism is higher than the temperature predicted using the GRI-Mech 3.0 mechanism at the steady-state stage. Similar to propane, the simulations of methane combustion with GRI-Mech 3.0 show that extinction occurs earlier than with the single-step mechanism, but the difference in ϕ-value at extinction is larger than for the propane cases.

Variations of the inflow equivalence ratio, ϕ_{in}

When testing how the PSR responded to variations at the inlet, we started with small variations in the inflowing equivalence ratio, cf. Cases 1 and 2 in Table 3. Figure 3 shows the results for propane and methane with a 2.5 % variation in $\bar{\phi}_{\text{in}}$. The results with a 5.0 % variation in $\bar{\phi}_{\text{in}}$ show the same, but with amplitudes of twice the size. The results for the global propane
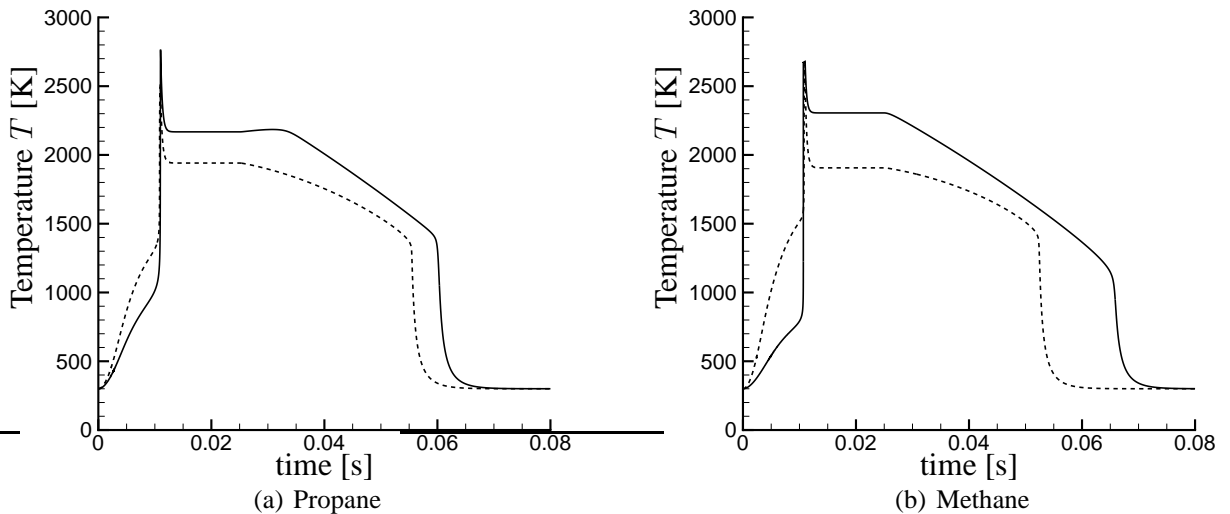
(a) Propane   (b) Methane

Figure 2: Ignition and extinction of propane and methane. Solid line: single step global mechanism. Dotted line: detailed mechanism.

mechanism are qualitatively in excellent accordance with the results reported in [2] and show that the reaction-rate oscillations increase significantly as the equivalence ratio decreases. As can be seen in Fig. 3 a, the amplitude of the oscillating reaction rate of propane goes to zero at $t \approx 0.15$ s when using the global single-step mechanism. From the mass fractions of C_3H_8 and O_2, temperature and density, it was observed that there is excess of propane leaving the reactor between $t = 0.05$ s and $t \approx 0.15$ s. This incomplete combustion is due to the short residence time. The reaction-rate oscillations were in phase with the C_3H_8 mass-fraction and the density oscillations, and out of phase with the O_2 mass fraction and temperature oscillations. The temperature reached its maximum at $t \approx 0.15$ s, the point where most of the fuel was consumed. Around $t \approx 0.15$ s, the C_3H_8 and O_2 mass-fraction oscillations started competing, the two being in opposite phases, and hence the resulting reaction-rate amplitude goes to zero. After $t \approx 0.15$ s, the incoming mixture was so fuel-lean that almost all C_3H_8 was consumed, and the resulting reaction-rate oscillations were in phase with the O_2 mass fraction and the density ρ. In this time-range ($t > 0.15$ s) the temperature decreased because the mixture was diluted with excess air and less fuel flowed into the reactor. Investigating Eq. (6) for the global propane mechanism, the variation in $Y_{C_3H_8}$ and temperature appear to neutralize each other giving a nearly constant reaction rate for the time interval 0.05 s to 0.15 s as Y_{O_2} and ρ were nearly constant. After this, almost all the fuel was consumed, the mass fraction of O_2 increased, the temperature decreased, density increased and the reaction rate decreases more or less linearly with time. From $t \approx 0.25$ s, the amplitude of the reaction-rate oscillation is constant. Testing for a longer residence time, $1/\tau = 100/\rho\,\mathrm{s}^{-1}$, the reaction rate for propane showed a more linearly decreasing development without the flat part in the beginning. This was because more of the propane was consumed at the steady-state stage.

Simulations with the detailed chemical mechanism shows a considerably different development, see Fig. 3 a. Here, oscillations of the propane reaction rate have an almost constant amplitude for the whole time-range.

From the corresponding simulations for methane, the transient developments of the CH_4 reaction rates were very similar for both the global and the detailed mechanism (GRI-Mech 3.0). Hence, only the result from the simulation with the global single-step methane mechanism is shown in Fig. 3 b. Because of the nature of the global mechanism (unit coefficients for Y_{O_2} and Y_{CH_4}) and some excess methane in the reactor for $t < 0.1$ s, the reaction rate is a bit damped due
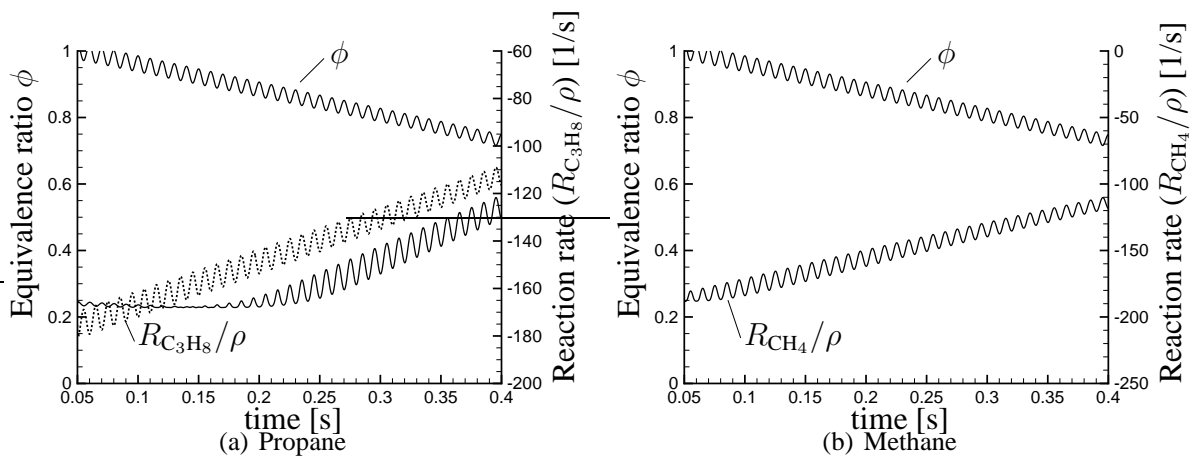
Figure 3: Reaction-rate response to a 2.5% variation in $\bar{\phi}_{\mathrm{in}}$. Solid line: single step global mechanism. Dotted line: detailed mechanism.

to too lack of O_2. For the remaining time-range, both the global and the detailed mechanisms give a methane reaction rate for which the oscillations have an almost constant amplitude. Figures 4 a-c show graphs of CO, CO_2 and OH reaction-rate oscillations due to a 5 % variation in $\bar{\phi}_{in}$ using the detailed mechanisms. The predicted results using the two detailed mechanisms show the same trends for each species. For both mechanisms the oscillations in reaction rate for CO_2 and OH increase with decreasing $\bar{\phi}_{in}$, while CO and H_2 (not shown, about 20 % of the mean reaction rate of OH) decrease. CO and H_2 have the same evolution in time. For $t < 0.12$ s the reaction-rate oscillations for OH are a bit damped. The amplitude of the reaction-rate oscillations for H_2O was nearly constant (not shown here, approximately 80 % of the mean reaction rate of CO_2). The reaction-rate response to the 2.5 % variation in $\bar{\phi}_{in}$ was similar, only with smaller amplitude (half the magnitude). Comparing Figs. 3 and 4 a-c, the large increase in reaction-rate oscillations seen when using the global propane mechanism is not predicted with the detailed mechanisms. The increase in the reaction rate for CO_2 is not as fast as predicted by the global propane mechanism, and the H_2O reaction-rate amplitude was constant. The global propane mechanism is clearly not reproducing all the features of the detailed mechanism.

Variations in inlet flow rate $\dot{m}_{in}/V_R$

Next, the reaction-rate responses to small-amplitude periodic inlet flow-rate variations were tested (see Eq. (12) and Table 3). Only results for propane with the global single-step mech-

(a) San-Diego mechanism

(b) San-Diego mechanism

(c) GRI-Mech 3.0

(d) Single step global mechanism
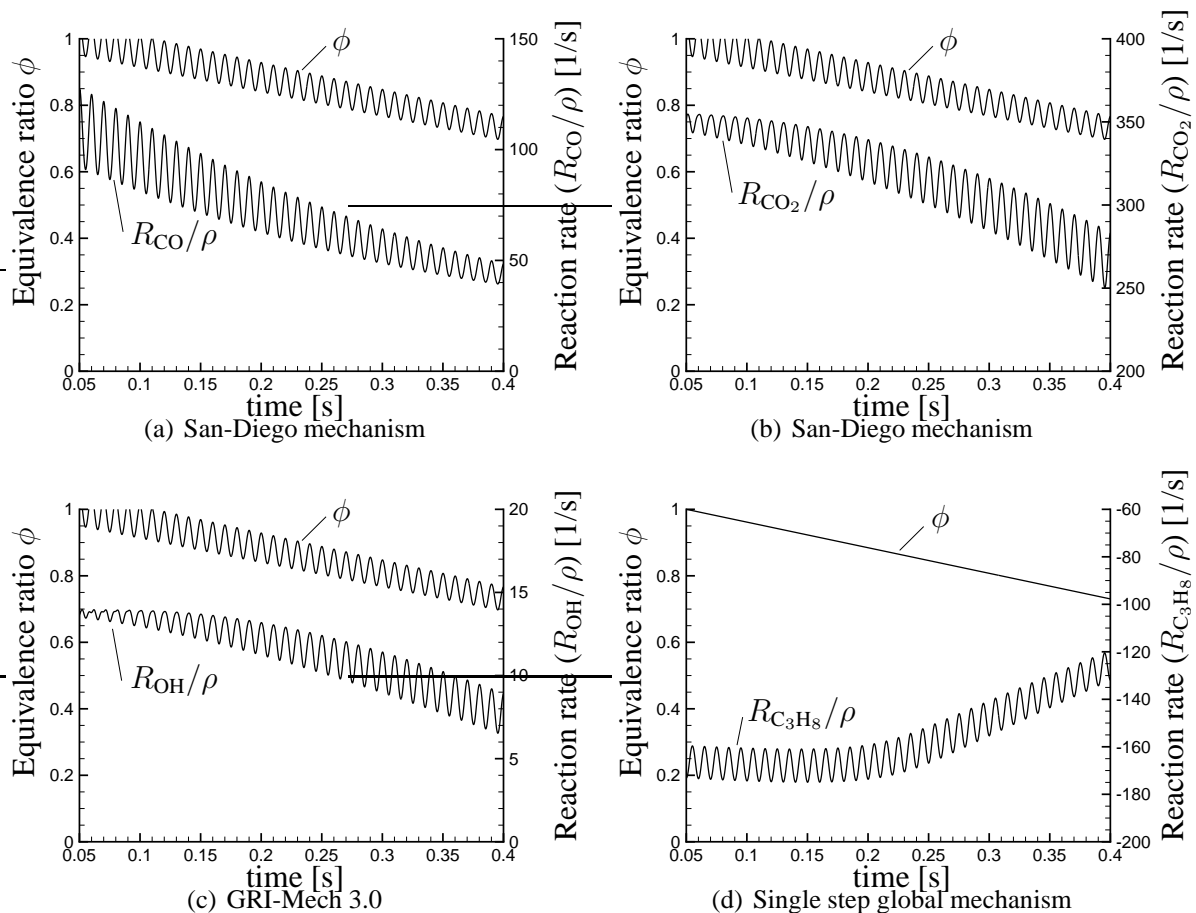
Figure 4: (a)-(c): Reaction-rate response to a 5% variation in $\bar{\phi}_{in}$. (d): Propane reaction-rate response to a 5% variation in $\dot{m}_{in}/V_R$

anism are shown in Fig. 4 d. The simulations with the two methane mechanisms showed that the mean reaction rate, R_{CH_4}/ρ [1/s], (not shown here) decreased linearly from about -170 to -100. Both mechanisms showed quite similar transient development. The reaction-rate oscillations, $R_{C_3H_8}/\rho$ [1/s], when using the detailed propane mechanism, decreased linearly from about -180 to -110. The reaction-rate oscillations amplitude decreased a bit as the mean equivalence ratio decreased, but the magnitude of the amplitudes were very similar to the global single-step propane mechanism. Also here the results of the global propane mechanism are in good agreement with the simulations reported by Lieuwen et al. [2]. The transient development of the C_3H_8 reaction rate shows a flat profile in the beginning, for the same reasons as when varying $\bar{\phi}_{in}$. Figure 4 d shows that the amplitude of the reaction-rate oscillations is nearly constant, only with a minor decrease at lean conditions. Lieuwen et al. [2], on the other hand, report a small increase in the amplitude when making the mixture leaner.

The reaction-rate oscillations for CO, CO_2, OH, H_2 and H_2O, due to a 5.0% variation in $\dot{m}_{in}/V_R$, were obtained from the detailed mechanisms. The different species oscillating reaction rates have the same transient trends as shown in Figs. 4 a-c and described in the previous section, but the amplitudes were almost constant, only with a small decrease as the mean equivalence ratio decreased.

The results from both global and detailed mechanisms indicate that combustion instabilities in premixed combustors from such variations remain unchanged with a decrease in $\bar{\phi}_{in}$.

Variations of inflowing temperature T_{in}

In the final test, the response of the reaction rates to periodic small-amplitude variations in the reactor inlet temperature was simulated (see Eq. (11) and Table 3). Such temperature oscillations could be due to for example acoustic disturbances or pressure fluctuations [2]. Also for this test, the response of the PSR model with the use of the global propane mechanism showed qualitatively the same behavior as in the work of Lieuwen et al. [2], that is a flat profile in the beginning. Variation of inlet temperature gave, for the global propane mechanism, a decrease in amplitude of the fuel reaction-rate oscillations (which were approximately 30 % of the amplitude shown in Fig. 4 d) as the mean equivalence ratio was decreased. Using the San-Diego mechanism the propane reaction-rate oscillations had a small, constant amplitude about a value linearly decreasing with decreasing equivalence ratio (approximately 25 % of the reaction-rate amplitude shown in Fig. 3 a).

The reaction rate of methane, from both the global and the detailed mechanism (GRI-Mech 3.0), had oscillations with small and constant amplitude (approximately 25 % of the reaction-rate amplitude shown in Fig. 3 b). Unlike the global propane mechanism there was no decrease in amplitude of the oscillations as the mean equivalence ratio was decreased. The reaction-rate responses of CO, CO_2, OH, H_2 and H_2O from the detailed mechanisms are not shown in this paper. The amplitudes of the reaction-rate oscillations due to varying the inlet temperature were quite small and constant, and the trends of the reaction rates were the same as shown in Figs. 4 a-c. On the other hand, the results predicted by the global propane mechanism suggest that combustors operating closer to stoichiometric conditions are more sensitive to combustion instabilities from such variations. However, the global propane mechanism gave unphysical results for ϕ_{in} close to stoichiometric conditions.

Discussion

The use of the global single-step mechanisms in this study has been done as a followup of the work of Lieuwen et al. [2]. These global single-step kinetic mechanisms have a range of validity that is usually quite limited [11, 12]. Either temperature ranges or equivalence ratios are specified, or both. The performance of the global mechanism in a open reactor depends very much on its parameters, as the species concentration coefficients, the activation energy and the pre-exponential collision frequency factor. As stated in [8], global mechanisms should be used with much care and only for engineering purposes as approximations. For the global mechanisms used in this study, different tests have been performed in order to check model validity. The methane mechanism has unit reaction orders, while the propane mechanism has reaction orders of 0.1 and 1.65 with respect to propane and oxygen. Whereas the methane mechanism worked for all the tests performed, the propane mechanism gave numerical problems for a wide range of equivalence ratios and reactor residence times, resulting in negative mass fractions and stop of the RADAU5 integrator.

When simulating variations of the inflowing equivalence ratio, the reaction-rate oscillations for OH were a bit damped for $t < 0.12$ s, see Fig. 4 c. Near the stoichiometric condition a variation of the inflowing equivalence ratio would alternatingly make the mixture rich and lean. For $\phi > 1$ the reaction-rate oscillations will not get larger than the value of the reaction rate at $\phi = 1.0$. As the mixture became leaner, the amplitude of the reaction-rate oscillations grew and became constant. The reaction-rate response of H_2 due to variations of the inflowing equivalence ratio was an amplitude that became smaller as the value of $\bar{\phi}_{in}$ was lowered. The main species of the hydrogen reactions is H_2O, for which the reaction-rate oscillations had constant amplitude. Comparing the consumption rate of CH_4 or C_3H_8 with the production rate of H_2O, it was found that consumption almost equals production. The production rates of OH and H_2 were small compared to H_2O. OH and H_2 are, among other, intermediate species for the production of H_2O. Without doing a thorough reaction path analysis, it is not clear how the different species react in order to produce H_2O based on the data shown in this paper. However, it seems that as the mixture gets richer on O_2, more from H_2 react with O to form OH. Comparing the production rate of CO and CO_2 with the consumption rate of CH_4 or C_3H_8, the sum is close to zero. CO and CO_2 are the main species among the carbon products. The same trends as for OH and H_2 are found when the mixture gets leaner. The amplitude of the reaction-rate oscillations decreased for CO as more O_2 were present, since CO most probably react faster with O to form CO_2. However, a reaction path analysis is needed to check this thoroughly.

In a gas turbine combustion chamber the inlet pressure and temperature can for example be 20 atm and 800 K, respectively. Conducting a simulation of methane with the GRI-Mech 3.0 mechanism, varying the inflowing equivalence ratio and using these conditions, we found that the reaction-rate trends were the same. However, reaction-path analysis may reveal some further differences.

Conclusions

A perfectly stirred reactor (PSR) model has been used to study reaction-rate responses to varying inlet mass flow rate, temperature and mixture equivalence ratio. Modeling the combustor as a perfectly stirred reactor, neglecting spatial effects, convection and mixing processes, makes it possible to isolate chemical kinetic effects, but simulations accounting for all relevant combustor processes are needed to give a clearer understanding of the complex nature of combustion instabilities.

For all simulations, the mixture is ignited at stoichiometric conditions. Then the mixtures are linearly made more and more lean while a small oscillation is imposed on one of the inlet variables. Global single-step and detailed chemical kinetic mechanisms have been used to study the combustion of methane and propane. The GRI-Mech 3.0 [14] and the San-Diego mechanism [15] have been used for simulating methane-air and propane-air combustion, respectively. The results show that the use of global single-step mechanisms for studying combustion at different equivalence ratios can lead to erroneous conclusions. A comparison of the performance of a single-step propane mechanism and the detailed San-Diego mechanism show that the global mechanism predicts almost zero decrease in the mean fuel consumption rate for decreasing equivalence ratios near stoichiometric conditions. On the other hand, the global methane mechanism and the detailed mechanisms showed a linear decrease in the mean fuel reaction rate for a decreasing equivalence ratio. When a small oscillation was imposed on the reactor temperature inlet, only small oscillations of the reaction rates are predicted. A similar oscillation imposed on the inlet mass flow rate gives larger amplitude oscillations that remain nearly constant for all equivalence ratios. Simulating the reaction-rate response to small oscillations in the equivalence ratio, both the global mechanism for methane and the detailed mechanisms predicted nearly constant amplitudes for the oscillating fuel consumption at both stoichiometric and lean conditions. The detailed mechanisms predicted that the reaction-rate oscillations, for other species than the fuel, had larger differences in the magnitude between stoichiometric and lean conditions. The simulations indicates that varying equivalence ratios play a role in driving combustion instabilities at lean conditions.

Acknowledgments

References

[1] T. Lieuwen and V. Yang, editors. *Combustion Instabilities in Gas Turbine Engines: Operational Experience, Fundamental Mechanisms, and Modeling*, volume 210. Progress in Astronautics and Aeronautics, 2005.

[2] T. Lieuwen, Y. Neumeier, and B. T. Zinn. The role of unmixedness and chemical kinetics in driving combustion instabilities in lean premixed combustors. *Combust. Sci. and Tech.*, 135:193–211, 1998.

[3] W. P. Shih, J. G. Lee, and D. A. Santavicca. Stability and emissions characteristics of a lean premixed gas turbine combustor. In *Twenty Sixth Symposium (International) on Combustion*, pages 2771–2778, 1996.

[4] J. M. Cohen and T. J. Anderson. Experimental investigation of near-blowout instabilities in a lean, premixed step combustor. American Institute of Aeronautics and Astronautics, 1996.

[5] T. Myhrvold and A. Gruber. Modelling of combustion instabilities with spider. research progress evaluation, unsteady reactor model, and further work. Technical Report TRA6300, SINTEF, Trondheim, Norway, 2006.

[6] T. Poinsot and D. Veynante. *Theoretical and Numerical Combustion*. Edwards, 2nd edition, 2005.

[7] I. S. Ertesvåg. *Turbulent flow and combustion (in Norwegian)*. Tapir Academic Publisher, Trondheim, Norway, 2000.

[8] S. R. Turns. *An Introduction to Combustion, Concepts and Applications*. McGraw-Hill, 2nd edition, 2000.

[9] E. Hairer and G. Wanner. *Solving Ordinary Differential Equations II: Stiff and Differential-Algebraic Problems*. Springer Series in Computational Mathematics. Springer-Verlag, 2nd rev. edition, 1996.

[10] E. Hairer and G. Wanner. Radau5: `http://www.unige.ch/~hairer/prog/stiff/radau5.f`, `http://pitagora.dm.uniba.it/~testset/solvers/radau5.php`. [online]. Last visited March 2007.

[11] C. K. Westbrook and F. L. Dryer. Simplified reaction mechanisms for the oxidation of hydrocarbon fuels in flames. *Combust. Sci. and Tech.*, 27:31–43, 1981.

[12] C. K. Westbrook and F. L. Dryer. Chemical kinetic modeling of hydrocarbon combustion. *Prog. Energy Combust. Sci.*, 10:1–57, 1984.

[13] K. K. Kuo. *Principles of Combustion*. John Wiley & Sons, 2nd edition, 2005.

[14] G. P. Smith, D. M. Golden, M. Frenklach, N. W. Moriarty, B. Eiteneer, M. Goldenberg, C. T. Bowman, R. K. Hanson, S. Song, W. C. Gardiner, Jr., V. V. Lissianski, and Z. Qin. Gri-mech 3.0: `http://www.me.berkeley.edu/gri_mech/`. [online]. Last visited March 2007.

[15] San-diego mechanism: `http://maeweb.ucsd.edu/~combustion/cermech/`. [online]. Last visited March 2007.

[16] R. J. Kee, F. M. Rupley, E. Meeks, and J. A. Miller. Chemkin iii: a fortran chemical kinetics package for the analysis of gasphase chemical and plasma kinetics. `http://www.ca.sandia.gov/chemkin/docs.html`. Technical Report UC-405 SAND96-8216, Sandia National Laboratories, Livermore Ca, 1996.

[17] Stanjan equilibrium calculator: `http://navier.engr.colostate.edu/tools/equil.html`. [online]. Last visited March 2007.

[18] T. Lieuwen. Private communication, 2007.

[19] S. Sannan. Literature survey on combustion instabilities. Technical Report TR F6076, SINTEF, Trondheim, Norway, 2004.

[20] A. P. Dowling and A. S. Morgans. Feedback control of combustion oscillations. *Annu. Rev. Fluid Mech.*, 37:151–183, 2005.

[21] T. Lieuwen. Modeling premixed combustion - acoustic wave interactions: A review. *Journal of Propulsion and Power*, 19:765–781, 2003.

[22] S. Park, A. Annaswamy, and A. Ghoniem. Heat release dynamics modeling of kinetically controlled burning. *Combustion and Flame*, 128:217–231, 2002.

[23] K. K. Venkataraman, L. H. Preston, D. W. Simons, B. J. Lee, J. G. Lee, and D. A. Santavicca. Mechanism of combustion instability in a lean premixed dump combustor. *Journal of Propulsion and Power*, 15:909–918, 1999.

[24] F. A. Williams. *Combustion Theory: The Fundamental Theory of Chemically Reacting Flow Systems*. The Benjamin/Cummings Publishing Company, 2nd edition, 1985.

[25] Chemkin 4.1: `http://www.reactiondesign.com`. Last visited March 2007.